Jyväskylän yliopiston julkaisuarkisto
Jyväskylä University Digital Archive

UNIVERSITY OF JYVÄSKYLÄ

This is an electronic reprint of the original article.
This reprint *may differ* from the original in pagination and typographic detail.

Author(s): Torgovkin, Andrii; Chaudhuri, Saumyadip; Ruhtinas, Aki; Lahtinen, Manu; Sajavaara, Timo; Maasilta, Ilari

Title: High-quality superconducting titanium nitride thin film growth using infra-red pulsed laser deposition

Year: 2018

Version:

Please cite the original version:

Torgovkin, A., Chaudhuri, S., Ruhtinas, A., Lahtinen, M., Sajavaara, T., & Maasilta, I. (2018). High-quality superconducting titanium nitride thin film growth using infra-red pulsed laser deposition. Superconductor Science and Technology, 31, Article 055017. https://doi.org/10.1088/1361-6668/aab7d6

All material supplied via JYX is protected by copyright and other intellectual property rights, and duplication or sale of all or part of any of the repository collections is not permitted, except that material may be duplicated by you for your research use or educational purposes in electronic or print form. You must obtain permission for any other use. Electronic or print copies may not be offered, whether for sale or otherwise to anyone who is not an authorised user.

Superconductor Science and Technology

ACCEPTED MANUSCRIPT

High-quality superconducting titanium nitride thin film growth using infra-red pulsed laser deposition

To cite this article before publication: Andrii Torgovkin *et al* 2018 *Supercond. Sci. Technol.* in press https://doi.org/10.1088/1361-6668/aab7d6

Manuscript version: Accepted Manuscript

Accepted Manuscript is "the version of the article accepted for publication including all changes made as a result of the peer review process, and which may also include the addition to the article by IOP Publishing of a header, an article ID, a cover sheet and/or an 'Accepted Manuscript' watermark, but excluding any other editing, typesetting or other changes made by IOP Publishing and/or its licensors"

This Accepted Manuscript is **© 2018 IOP Publishing Ltd**.

During the embargo period (the 12 month period from the publication of the Version of Record of this article), the Accepted Manuscript is fully protected by copyright and cannot be reused or reposted elsewhere.
As the Version of Record of this article is going to be / has been published on a subscription basis, this Accepted Manuscript is available for reuse under a CC BY-NC-ND 3.0 licence after the 12 month embargo period.

After the embargo period, everyone is permitted to use copy and redistribute this article for non-commercial purposes only, provided that they adhere to all the terms of the licence https://creativecommons.org/licences/by-nc-nd/3.0

Although reasonable endeavours have been taken to obtain all necessary permissions from third parties to include their copyrighted content within this article, their full citation and copyright line may not be present in this Accepted Manuscript version. Before using any content from this article, please refer to the Version of Record on IOPscience once published for full citation and copyright details, as permissions will likely be required. All third party content is fully copyright protected, unless specifically stated otherwise in the figure caption in the Version of Record.

View the article online for updates and enhancements.

This content was downloaded from IP address 130.234.75.189 on 20/03/2018 at 12:21

High-quality superconducting titanium nitride thin film growth using infra-red pulsed laser deposition

A Torgovkin[1]‡, S Chaudhuri[1]§, A Ruhtinas[1], M Lahtinen[2], T Sajavaara[3] and I J Maasilta[1]

[1] Nanoscience Center, Department of Physics, University of Jyväskylä, P. O. Box 35, FIN-40014 University of Jyväskylä, Finland

[2] Department of Chemistry, Laboratory of Inorganic and Analytical Chemistry, P.O. Box 35, FIN-40014 University of Jyväskylä, Finland

[3] Accelerator Laboratory, Department of Physics, University of Jyväskylä, P. O. Box 35, FIN-40014 University of Jyväskylä, Finland

E-mail: maasilta@jyu.fi

Abstract. Superconducting titanium nitride (TiN) thin films were deposited on magnesium oxide, sapphire and silicon nitride substrates at 700°C, using a pulsed laser deposition (PLD) technique, where infrared (1064 nm) pulses from a solid-state laser were used for the ablation from titanium target in a nitrogen atmosphere. Structural studies performed with X-ray diffraction showed the best epitaxial crystallinity for films deposited on MgO. In the best films, superconducting transition temperatures, T_C, as high as 4.8 K were observed, higher than in most previous superconducting TiN thin films deposited with reactive sputtering. A room temperature resistivity down to $\sim 17\mu\Omega$cm and residual resistivity ratio (RRR) up to 3 were observed in the best films, approaching reported single crystal film values, demonstrating that PLD is a good alternative to reactive sputtering for superconducting TiN film deposition. For less than ideal samples, the suppression of the film properties were correlated mostly with the unintended incorporation of oxygen (5 – 10 at. %) in the film, and for high oxygen content films, vacuum annealing was also shown to increase the T_C. On the other hand, superconducting properties were surprisingly insensitive to the nitrogen content, with high quality films achieved even in the highly nitrogen-rich, Ti:N = 40/60 limit. Measures to limit oxygen exposure during deposition must be taken to guarantee the best superconducting film properties, a fact that needs to be taken into account with other deposition methods, as well.

Keywords: titanium nitride, pulsed laser deposition (PLD), elemental analysis

PACS numbers: 74.62.Bf, 74.70.Ad, 74.25.fc, 81.15.Fg, 61.05.cp

Submitted to: *Supercond. Sci. Technol.*

‡ Present address: BlueFors Cryogenics Oy, Arinatie 10, FI-00370 Helsinki, Finland

§ Present address: Picodeon Ltd Oy, Piisilta 1, FI-91100 Ii, Finland

Accepted Manuscript

1. Introduction

Titanium nitride (TiN) as a thin film is of paramount technological importance because of its excellent electrical and mechanical properties, and chemical and thermal stability. It has been extensively used as a hard coating for wear resistance purposes in tools [1], as a gold-colored decorative layer [2] and as an optical coating [3]. In microelectronic industry it finds several applications, for example as a diffusion barrier [4] and as a gate electrode [5]. More recently, it has also been applied at low temperatures in superconducting devices such as microwave kinetic inductance detectors [6, 7, 8, 9, 10, 11, 12], microwave resonators [13, 14], quantum bits [15, 16] and tunnel junctions [17]. The advantage of TiN over more traditional materials such as Al and Nb has been reduced losses, leading to improvements in coherence times in qubits and improved sensitivity in detectors. Another potentially important application of superconducting TiN thin films is in the development of normal metal-insulator-superconductor (NIS) tunnel junction devices for thermometry and cooling[18], where TiN can offer a higher operational temperature range compared to Al. Lastly, TiN is also interesting material for the studies of superconductor-insulator transition in the limit where the films are disordered [19, 20, 21, 22, 23, 24].

Due to the wide range of applications, TiN films have been grown for decades on a variety of substrates using a broad variety of techniques ranging from chemical vapor deposition [25, 26] and atomic layer deposition (ALD) [27] to reactive sputtering [28, 29] and pulsed laser deposition (PLD) [30, 31], with reactive sputtering being the most common method. For superconducting applications, however, only ALD and reactive sputtering have been widely used, the former mostly for ultrathin, disordered film deposition for the superconductor-insulator studies, and the latter for the detector and qubit applications. The ALD deposited superconducting films [23, 32, 33] have typically had higher room temperature resistivities $\rho \sim 100 - 400\mu\Omega$cm and lower critical temperatures $T_C \sim 1.4$ – 3.6 K, whereas with reactive sputtering one typically can obtain ρs down to $\sim 20 - 30\mu\Omega$cm [14, 34] and T_C:s of 4.5 – 4.6 K [6, 35, 14, 34], if the nitrogen composition is close to stoichiometry. A few results also exist, where ultrahigh-quality epitaxial superconducting TiN films were successfully deposited either on Si with reactive sputtering [36] or on MgO substrates with molecular beam epitaxy [37], achieving high T_Cs around 5.3 – 5.4 K and low $\rho \sim 10 - 15\mu\Omega$cm with residual resistivity ratio (RRR) as high as 3 – 4. The highest reported bulk T_C for single crystal TiN in the literature is 6.0 K [38].

Although there is a fairly wide literature on PLD fabrication of TiN films, no reports on superconducting PLD grown films exist. However, high quality epitaxial TiN films have been produced by UV excimer laser PLD, mostly on Si (100) and (111) substrates [39, 40, 41, 42], but also on MgO [43, 44] and (0001) sapphire [45]. Infrared (IR) lasers at 1064 nm have also been used in PLD deposition of TiN [46, 47], but only polycrystalline films were deposited on metallic substrates at room temperature.

Recently, we have been able to grow high quality PLD superconducting NbN [48, 49]

Accepted Manuscript

and TaN [50, 51] thin films using IR pulses from a solid-state laser for ablation from elemental targets in nitrogen atmospheres. The advantages of using a solid state IR laser are its low operation costs, compactness and lack of corrosive gas hazards (in contrast to excimer lasers). For both NbN and TaN, we were able to achieve T_Cs close to the corresponding highest reported values.

In this paper, we report, for the first time, the fabrication of high-quality superconducting TiN thin films with a PLD technique using 1064 nm IR pulsed laser. The highest T_C observed was 4.8 K, higher than in most previous studies. Best results were obtained for films on MgO substrates, on which epitaxial growth was achieved. In the highest quality epitaxial films, room temperature resistivities down to $\sim 17\mu\Omega$cm and RRR up to 3 were obtained - results that are on-par with the highest quality sputtered single crystal films [29, 36]. Composition analysis with the help of Time-of-Flight Elastic Recoil Detection Analysis (ToF-ERDA) demonstrated a strong correlation between the oxygen impurity content the T_C and ρ, with low oxygen content producing a higher T_C and a lower ρ.

2. Experimental details

2.1. PLD deposition

TiN_x thin films were grown on three distinct substrates: cubic (100) oriented MgO (Crystec GmbH), hexagonal r-plane sapphire (Al_2O_3) (Crystec GmbH) and amorphous silicon nitride (SiN). The SiN layer ($\sim$ 300 nm thick) was grown on top of silicon (100) substrates using LPCVD. A rotating Ti target (99.999 % , Goodfellow Inc.) was ablated in an ultra high purity nitrogen atmosphere (99.99999 % purity) using 1064 nm (4 ns pulse width) laser radiation from a Q-switched Nd:YAG laser (EKSPLA Model: NL301 HT) operated at 10 Hz. The details of the 1064 nm radiation based PLD technique can be found elsewhere [50, 52]. The target to substrate distance was 5 cm while the areal energy density of the pulse incident on the Ti surface was $\sim$ 6 Jcm^{-2}. The base vacuum ranged between 3 – 8 $\times 10^{-6}$ mTorr, when chamber was turbopumped during the substrate temperature ramp-up (2 h), but could be pushed as low as 3×10^{-7} mTorr after a procedure of chamber baking and flushing with nitrogen was employed. This improvement was obtained by pumping the chamber with a turbomolecular pump for 12 hours with a constant flow of nitrogen (1.0 sccm), and keeping the substrate heater hot at 700 – 770 °C. The baking presumably leads to increased outgassing from the chamber, reducing the deleterious oxygen outgassing during film deposition. As will be seen later, this is a critical step to produce higher quality superconducting TiN films.

During deposition, the substrate temperature was held at 700 °C and the films were deposited in a constant flow of nitrogen. In order to vary the Ti:N ratio, films were grown at several flow rates between 0.08 and 10.0 sccm. Before the actual deposition run, pulses were first fired with a shutter closed for several minutes so that surface oxides and contaminants from the target material did not reach the substrate. After the shutter

Accepted Manuscript

was opened, in each deposition run approximately 12000 laser shots were fired which resulted in film thickness varying between 32 – 175 nm corresponding to a growth rate of $\sim 0.3 - 1.5$ Å/sec. This variation in the growth rate results most likely from variations in the nitrogen flow, position of the laser on the target, the depth of the target groove etc., which all affect the plasma dynamics and thus deposition rate; run-to-run consistency with constant conditions is nevertheless possible. After deposition, the films were let to cool back to room temperature in a constant flow of high-purity nitrogen at the same flow rate as the deposition flow rate, with the temperature ramping down at a rate of 5 °C per minute. In addition, several films deposited at the flow rates corresponding to highest T_C region were chosen to be post-annealed in vacuum. Annealing took place in the same deposition chamber, without breaking the vacuum. The deposition chamber was pumped to base pressure with a turbomolecular pump while the temperature of the substrates was ramped up to 770 °C in 2 h. After reaching the maximum temperature, it was immediately ramped down to room temperature again in four hours.

2.2. Device fabrication and electrical measurements

Using electron-beam lithography (EBL) and reactive ion etching (RIE), the films were patterned to obtain a Hall bar geometry. The length and width of the Hall bars were 500 μm and 100 μm, respectively, and the film thicknesses (t) were determined using an atomic force microscope after patterning. For films deposited without chamber baking, a layer of evaporated copper was used as an etch mask while a mixture of CHF_3 and O_2 gas served as the etchant in RIE. This patterning recipe is identical to that used for TaN film etching, as described in more detail in Ref[51]. For films deposited with the chamber baking procedure, no copper was used, instead $\sim$ 400 nm PMMA resist served as the etch mask for an SF_6 (100 sccm) and O_2 (2 sccm) RIE etch with 60 W power.

Longitudinal and Hall resistivity measurements were carried out in the standard four probe configuration for Hall bar devices, wire bonded onto a sample stage that could be cooled down. The devices with low T_Cs were mounted in a 1-K pot refrigerator, while the samples with T_Cs higher than 4.2K were measured with a He4 dipstick. The temperature dependence of the resistivity was recorded with an AC resistance bridge (AVS-47) as well as with a lock-in technique, using a bias current of 1 μA at 17 Hz as the excitation. For Hall measurements, the devices were mounted in a dipstick, surrounded by a superconducting solenoid and immersed in liquid helium. DC biasing with a current of 1.2 mA was used, with the current constantly monitored using a current pre-amplifier (Ithaco 1211). The Hall and longitudinal voltages were recorded as a function of the applied magnetic field, using low noise voltage pre-amplifiers (Ithaco 1201).

2.3. Structural and compositional analysis

Structural analysis of the TiN thin films were carried out at room temperature using X-ray diffraction (XRD) in the traditional Θ-2Θ scanning configuration. The diffractograms were recorded by PANalytical X'Pert Pro alpha 1 diffractometer using

Accepted Manuscript

Johansson monochromatized Cu $K_{\alpha 1}$ radiation ($\lambda = 1.5406$; tube settings: 45 kV, 30 mA). Each thin film plate was prepared onto a silicon-made zero-background signal producing holder having adequate sample cavity that matches to the plate thickness. The data was collected from a spinning sample by XCelerator detector in the 2Θ-range of 20 – 100° with a step size of 0.017° and counting times of 120 s per step. The diffraction data was worked by XPert HighScore Plus v. 2.2d software package and the ICDD PDF 4+ powder diffraction database was used for the qualitative search-match phase identification.

The composition analysis was done with the help of time-of-flight - energy spectrometer (Tof-ERDA) for elemental depth profiling. A beam of either 13.615 MeV $^{63}Cu^{7+}$ or 11.915 MeV $^{63}Cu^{6+}$ was chosen to irradiate the films at 20° or 10° angle, and the recoil atoms were analyzed at an angle of 41° with respect to the incoming beam [53]. Heavy ions were chosen in order to effectively knock out Ti atoms from the film and thus keep the total ion fluence low, saving films from excessive radiation damage.

3. Results

3.1. Surface topography and crystal structure

The surface topography of some TiN thin films was investigated using scanning electron and atomic force microscopy, with representative micrographs displayed in Fig. 1. Both the SEM and AFM images reveal a relatively uniform surface with very low particulate density (sometimes particulates are an issue with PLD deposition) with a grain size ranging from $\sim 10 - 50$ nm. The root mean square surface roughness values are low, in a range $1.2 \sim 3$ nm. Such smooth surfaces are welcome for device fabrication, such as micron-scale tunnel junctions, as was already demonstrated for superconducting NbN and TaN films grown in the same deposition chamber [48, 51]. The grain size on MgO is larger than on SiN and sapphire, pointing to a difference in the crystallography of the growth, in agreement with the XRD data discussed below.

The X-ray diffractograms of TiN films grown on (100) MgO (no pre-baking) at different nitrogen pressures p_N are displayed in Fig. 2(a). We see that the diffractograms are dominated by the (200) and (400) MgO substrate peaks at 43° and 94°. Next to the MgO peaks (on the left hand side), the respective strong TiN peaks at 42.6° (200) and 92.7° (400) are visible, indicating epitaxial growth. Such an epitaxy is expected and has been observed before [43, 44, 37, 54], as both MgO and TiN have a cubic rocksalt structure, and the bulk lattice mismatch is only $\sim 0.6\%$ [38, 44]. The full range of 2Θ is shown in Fig. 2(b), showing that no other phases or orientations are seen; most notably, the other possible low energy orientation, the (111) peak at 36.7° often seen in polycrystalline films [14, 36] is absent. From Fig. 2 (a), an evolution of the crystal structure with p_N is also visible. The position of the maxima of the TiN peaks and hence the out of plane lattice parameter c increases with p_N. This variation is also displayed in Fig. 2 (a), inset. The dependence is approximately linear with a slope of $\sim$

Accepted Manuscript

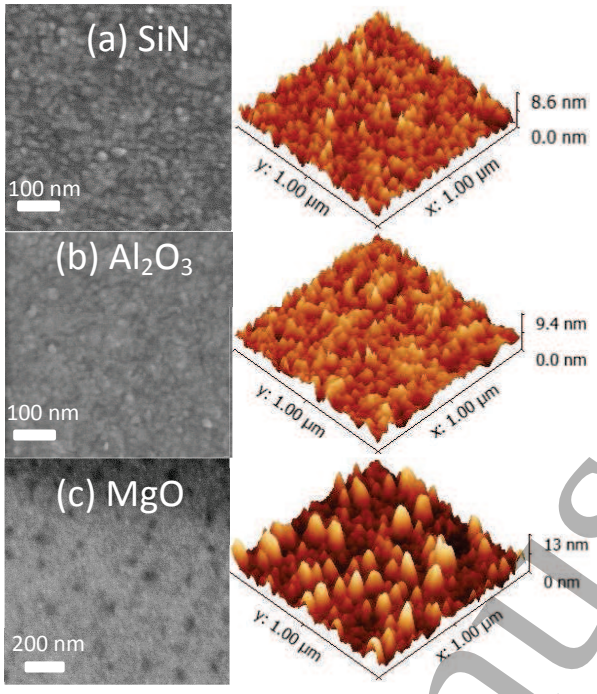

Figure 1. Room temperature scanning electron (left panel) and atomic force (right panel) micrograph of TiN films grown on (a) SiN (b) sapphire and (c) MgO at 32 mTorr of nitrogen pressure. The scale of the scanning electron micrographs are indicated by the horizontal white line on bottom left. The scan area for the atomic force micrographs was 1×1 μm^2. All the AFM films were deposited at $p_N = 77$ mTorr ($f_N = 5.5$ sccm).

1pm/mTorr.

In Fig. 2 (b), in addition to the MgO substrate sample, the diffractograms of TiN films grown on Si/SiN and sapphire are also shown. All films were deposited at the same $p_N = 77$ mTorr without chamber baking and have nearly the same thickness. As expected, due to the large lattice mismatch between TiN and r-cut sapphire and the amorphous nature of the SiN, there are no strong TiN reflections in the corresponding films. The TiN grown on sapphire and SiN is polycrystalline in nature. Only very weak signals from the (200) TiN peaks are visible in both films, in addition to a weak signatures of (220) TiN peaks (61.9° 2Θ).

In addition to structure studies on as-deposited films, we have also investigated the effect of post-deposition annealing of polycrystalline films. In Fig. 2 (c), an example of diffractograms of a pair of annealed and non-annealed TiN films grown on top of Si/SiN are shown. Several pairs of films were grown one right after another at $p_N = 77$ mTorr and only on SiN substrates, minimizing possible oxygen or water release to the film from the substrate during annealing. In the case of non-annealed film (black line), two cubic TiN diffraction peaks are observed at 42.6° and 61.9° 2Θ, again the (200) and (220) peaks of cubic rocksalt TiN. In the case of the annealed film (red line) the two peaks remain, but the (200) peak gets stronger, indicating improved crystallinity. However, it was never possible to obtain a single orientation, i.e. a transition from

Accepted Manuscript

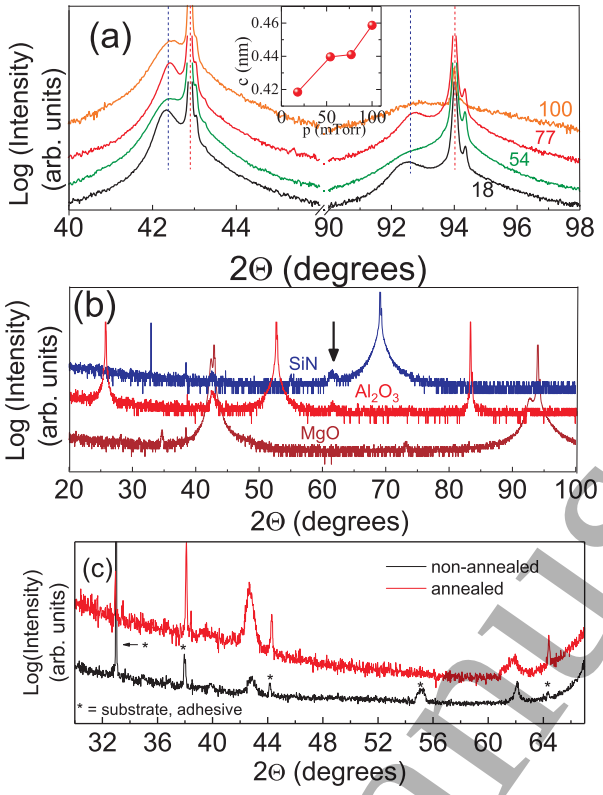

Figure 2. (a) Left: Θ-2Θ X-ray diffractograms of TiN films deposited on (100) oriented MgO substrates at different nitrogen pressures (in mTorr) indicated by the numbers. The expected characteristic positions of the TiN (200) and (400) peaks are indicated by the blue dashed lines. Inset: The variation of the out of plane lattice parameter of the films with nitrogen pressure during deposition. Non-relevant 2Θ-range of from 46° to 90° was cut by the axis break. (b) X-ray diffractograms of TiN films with nearly identical thicknesses deposited on different substrate at 77 mTorr. The position of the weak (220) TiN peak on sapphire and SiN is marked by an arrow. (c) X-ray diffractograms of the annealed (red line) and non-annealed (black line) TiN films on SiN/Si. Peaks marked with asterisk are recognized as originating from the substrate or silver adhesive.

polycrystallinity to a more oriented film. In some annealed samples (not shown), some new peaks appeared, indicating increasing polycrystallinity and/or appearance of new phases.

From AFM measurements, we could also see a roughening of the sample surface after the anneal, where the rms roughness increased from ~ 2 nm up to 4.6 nm.

3.2. Electrical characterization of superconducting properties

For all samples the resistivity of the films was measured as a function of temperature. Even without pre-baking of the chamber, superconducting transitions were observed on all substrates used, MgO, sapphire and SiN. The qualitative behavior of the resistivity vs temperature curves was always the same in this case – a small ~ 10 % decrease of ρ down to ~ 50 K, a temperature independent region, and finally a superconducting

Accepted Manuscript

transition around 3 K. ρ did not depend strongly on substrate either, being typically around 80 - 100 $\mu\Omega$cm. Compared to sputtered films [6, 35, 14, 34], the obtained T_Cs in this case are somewhat lower, with ρs in the same range. However, the results are quite similar to high quality ALD films of similar thickness range [23, 32]. Interestingly, the higher crystallinity of the films on MgO was not reflected in higher T_C; other factors influence the superconducting properties more strongly, as will be clearer later.

Superconducting transitions were also measured for two sample pairs on SiN substrates, where both of them were deposited with identical conditions, but one of them was was post-annealed, as described in Section 2. In both pairs (deposited at pressures p_N = 77 mTorr and 91 mTorr), the non-annealed samples showed somewhat low transitions with T_C = 2.5 K, but the annealed samples had much higher T_Cs of 3.2 K and 3.8 K. There is thus evidence from both structural and electrical measurements that the properties of less-than-ideal films can be improved by such post-deposition annealing.

On the other hand, some materials are known to be quite sensitive to the chamber conditioning before deposition. Therefore, we also deposited a set of films with pre-baking of the chamber, as described in section 2. The parameters for those films are shown in Table 1, and some resistivity vs. temperature curves in Fig. 3. For these depositions MgO substrates were used, and nitrogen flow rate (and thus pressure) was varied. What is strikingly clear from Table 1 is that the T_Cs are now significantly higher, ranging up to 4.83 K in the best case. Correlated with this increase, there is a clear trend of much lower resistivities than in the films deposited without pre-baking. In the film with the highest T_C (7.7 sccm flow), the resistivity is as low as 5.72$\mu\Omega$cm at 4.2 K, which corresponds to a room temperature resistivity of 17.7 $\mu\Omega$cm. Both these T_C and ρ are exceptionally good, on-par with the highest quality sputtered single crystal films [29, 36]. Zooming into the transition regions [Figs. 3(b)-(d)], we observe that the transitions are quite narrow, down to a width 10 mK in the best cases, indicating quite uniform superconducting properties.

Although all data in Table 1 is for MgO substrates, we also deposited one film on SiN in the same exact run as the MgO film at 5.15 sccm nitrogen flow with T_C = 4.58 K. The obtained T_C on SiN was as high as 4.55 K, essentially the same as on MgO, showing that the substrate has little impact on the superconducting transition temperature. This is promising for device fabrication point of view, as nitridised silicon is much easier to work with than MgO in terms of device fabrication.

The films grown with pre-baking show much higher residual resistivity ratios (RRR) (Table 1), determined as the ratio of the film resistivity at room temperature to that at 4.2 K. Without pre-baking RRR was always close to one, in contrast, using pre-baking we have achieved RRR over three in the best case. As RRR is a measure of the quality of the films, we can safely conclude that pre-baking gives superior results. Thus, TiN as a superconducting material seems to be very sensitive to the deposition purity conditions, in our experience more so than NbN and TaN, the other two nitride superconductors we have deposited in our PLD chamber.

Accepted Manuscript

Table 1. Parameters of the TiN thin films deposited with chamber pre-baking. Here f_N and p_N are the nitrogen flow rate and pressure in the deposition chamber, t the film thickness, T_C the superconducting transition temperature , ρ the electrical resistivity at 4.2 K, and RRR the residual resistivity ratio.

Nitrogen			MgO		
f_N	p_N	t	T_C	ρ	RRR
sccm	mTorr	nm	K	$\mu\Omega$cm	
0.8	22	67	2.45	42.9	1.24
1.5	32.1	108	4.09	14	1.91
2.35	43.2	100	3.96	15.46	1.75
3.5	58.5	32	3.33	11.62	1.48
4.55	67.7	59	3.69	20.55	1.64
5.15	72.5	105	4.58	8.11	2.31
5.35	75.6	81	4.32	11.1	1.67
7.0	93	63	4.60	14.7	2.34
7.7	97.8	100	4.83	5.72	3.10
8.5	105	72	4.32	7.54	2.58

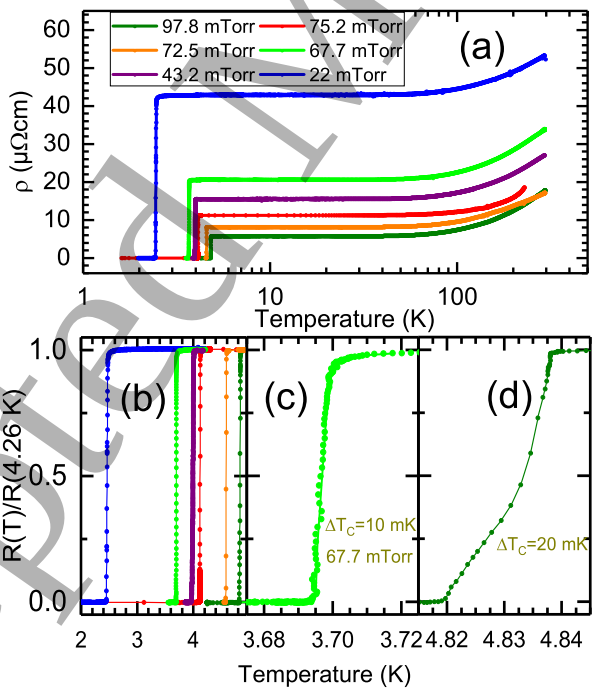

Figure 3. (a) Temperature dependence of the resistivity of selected TiN films grown on MgO after chamber baking at different p_N. Residual resistivity ratio is much higher than without baking. Sharp superconducting transition is seen in all films (b). ΔT_C was found to be as low as 10 mK (c), a bit higher ($\sim$ 20 mK) in the highest T_C film (d).

Accepted Manuscript

Looking at the results more carefully, Fig. 3(a) shows a clear correlation between the T_C and resistivity. This is plotted in Fig. 4 (a), with the dependence of T_C on the RRR plotted in Fig. 4 (b). A lower resistivity and a higher RRR, both indicating higher quality of the films, lead to a higher T_C. The outlier point in Fig. 4 (a) ($T_C = 3.3$ K, $\rho = 11.6\mu\Omega$cm) corresponds to a sample with a much thinner film (~ 30 nm) than the rest, thus the additional suppression of T_C could be a result of a direct influence the low value of the film thickness. Interestingly, though, that same data point falls in line with the rest when plotted as a function of RRR [Fig. 4 (b)], indicating that RRR correlation is even stronger.

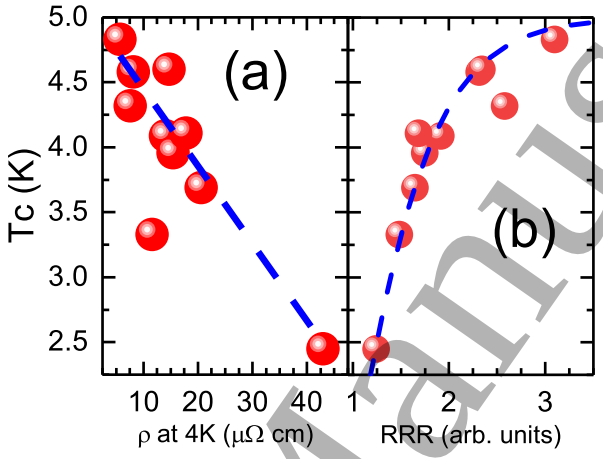

Figure 4. The dependence of T_C over the (a) 4 K resistivity and (b) residual resistivity ratio (RRR) of TiN films grown on MgO after chamber baking. The dashed lines are guides to the eye.

Let us now turn to the question, whether the film properties can be tuned by the nitrogen flow rate and/or pressure. First of all, in the PLD deposition, as opposed to sputtering, the two variables are not independent but strongly linearly correlated (Table 1), as no argon is involved in the plasma. In previous studies with reactively sputtered superconducting TiN films [6, 35, 14], a strong dependence on the nitrogen flow rate was seen, where low flow rates led to suppressed T_Cs, with a sharp transition. This was correlated with a phase transition from low-T_C nitrogen poor Ti_2N phase to a stochiometric, high-T_C TiN phase [35, 14]. We plot the dependence of T_C and ρ on the deposition nitrogen pressure in Fig. 5 (a) and (b), respectively, for all films deposited (including films without the pre-baking step).

The big picture from Figs. 5 (a) and (b) is that, although some variations are visible, no transition from low T_C to high T_C is seen, in contrast to the results on sputtered films [14, 35]. This is because our setup never produces strongly nitrogen deficient, substochiometric films even with the lowest flow rates, as will become clear later after discussing the compositional analysis. In addition, the obtained results are fairly insensitive to nitrogen pressure. This is in contrast to NbN [55] and TaN [50] films grown in the same chamber, for which the highest T_C superconducting films

Accepted Manuscript

were obtained in a much narrower range of nitrogen pressure. This difference can be understood, as the superconducting rocksalt δ-TiN phase is stable in a much larger range of nitrogen compositions away from perfect stoichiometry [56], as compared to the corresponding TaN and NbN phases. The only clear trend visible in Figs. 5 (a) and (b) is that in the films deposited with chamber baking, higher pressures produced higher T_Cs and slightly lower ρs on average. The strong improvements to the film quality (higher T_C, lower ρ) with the pre-baking step are clearly seen.

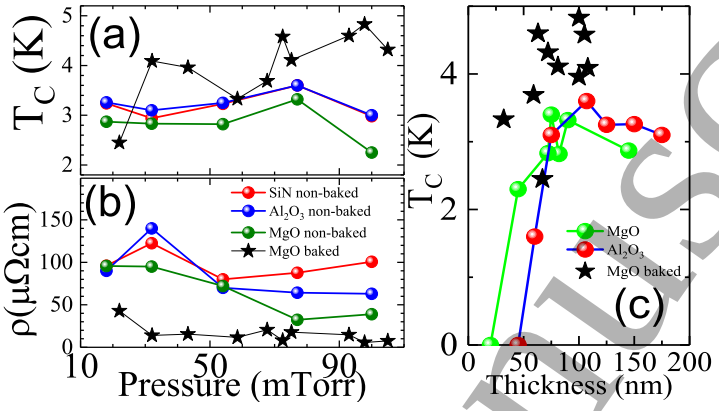

Figure 5. Variation of (a) the superconducting transition temperature and (b) the 4.2 K resistivity of TiN films as a function of nitrogen pressure, deposited on various substrates. (c) Thickness dependence of the superconducting transition temperature of TiN films deposited on MgO and Al_2O_3. The data for the set of films deposited with chamber baking are plotted in black.

In Fig. 5 (c), we also plot data as a function of thickness. For the films deposited without pre-baking, the T_Cs were found to be thickness dependent if the thickness was below $\sim$ 70 nm, for both MgO and sapphire substrates. For the thinnest 20 nm film on MgO and 45 nm film on Al_2O_3 no T_C was observed down to 0.08 K. However, using pre-baking, the thinnest film fabricated (30 nm) still had a T_C as high as 3.3 K.

3.3. Hall effect and magnetoresistance

For a set of TiN films on MgO deposited without pre-baking, we also measured the Hall (R_{xy}) and magnetoresistance (R_{xx}) in the normal state. Fig. 6(a) shows the variation of the Hall resistance of a TiN film grown on MgO at 54 mTorr as a function of the perpendicular applied magnetic field B measured at 4.2 K. The dependence is linear, as expected, and from the slope [$R_{xy} = B/(ne)$] we can calculate the effective charge carrier density n, which is n-type (electron dominated) for all films studied. Variations from film to film were observed, but in all cases a carrier density $n \sim 4 - 6 \times 10^{22}\text{cm}^{-3}$ was measured. This result is in agreement with the literature result $5 \times 10^{22}\text{cm}^{-3}$ from sputtered single crystal films [29], and around the theoretical conduction electron density of [57] $5.25 \times 10^{22}\text{cm}^{-3}$.

The evolution of the longitudinal magnetoresistance of the same film is shown in Fig. 6(b). As is clearly seen, the magnitude of the magnetoresistance is quite small.

Accepted Manuscript

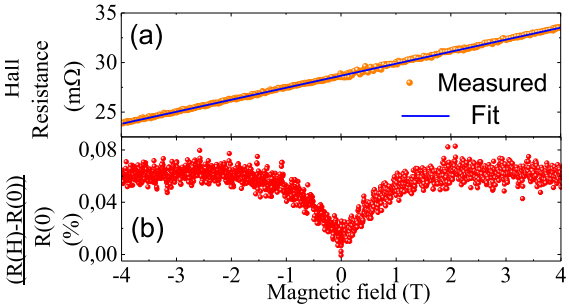

Figure 6. Variation of (a) Hall resistance and (b) longitudinal magnetoresistance of a TiN film deposited on MgO at 54 mTorr. The straight line in (a) is a linear fit to the data with a slope of 1.2 mΩ/Tesla. The offset in (a) is due to the influence of the longitudinal resistivity because of imperfect alignment of the Hall voltage leads. Similarily, in (b) a linear background was subtracted due to the partial coupling of ρ_{xy} into the longitudinal voltage.

Interestingly, linear variation is seen at low fields, as well as a saturation around 1 – 2 T, contrary to the behavior in simplest free-electron metals [58].

3.4. Compositional analysis

Finally, we subjected some of the deposited films to an analysis of their elemental composition using ToF-ERDA [53]. Examples of elemental depth profiles obtained are shown in Fig. 7, where a film deposited without pre-baking at p = 77 mTorr on SiN with a T_C = 2.57 K is shown in Fig. 7 (a), and a film deposited with pre-baking and a similar nitrogen pressure p = 71 mTorr on MgO with a T_C = 4.58 K in Fig. 7 (b). The two results are clearly very different, so conditioning of the chamber has a major impact on the elemental composition. First of all, one can see that the Ti/N ratio of the first film in (a) is very close to 1:1, so that the film is "stoichiometric", whereas the films deposited with pre-baking are much more nitrogen rich (Ti/N ratio $\sim$ 0.8). This is noteworthy, considering that the nitrogen flow was almost the same. Another big difference seen is the level of oxygen in the two films, which is as high as $\sim$ 11 at. % in the first film (no baking), but as low as 1 at. % in the second film (with baking). Clearly, pre-beaking the chamber gives a much lower oxygen impurity content, considering that an oxygen content at or below 1 at. % was seen in all analysed films deposited using pre-baking with a reasonable nitrogen flow rate, whereas without it the oxygen content varied between 5 at. % and 11 at. %. Typical surface impurities (C,H,O) are also seen in both samples. In the interior of the films, carbon and hydrogen impurities were always found, C typically below 1 at. % and H below 0.2 at. %.

In the above example, it seemed that low oxygen content and high nitrogen content were correlated with high T_C. To study this more, we plot how the measured T_C depends both on the Ti:N ratio (a) and on the oxygen content (b) in Fig. 8 for films deposited without chamber baking, where the oxygen content and its variation was larger. The nitrogen flow conditions were kept in the range 80 – 90 mTorr for all the films so that the

Accepted Manuscript

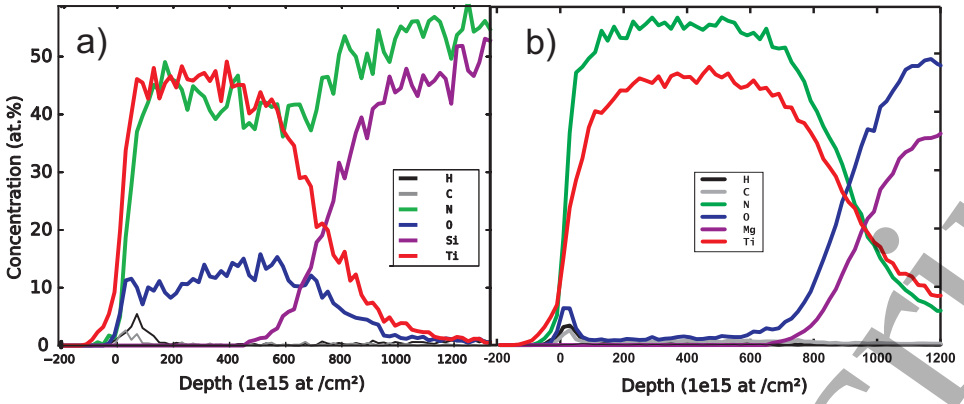

Figure 7. (a) The elemental depth profile of TiN film with the highest oxygen content, deposited on silicon nitride without chamber baking at p_N (f_N)= 77 mTorr (5.5 sccm). It has a T_C = 2.57 K. (b) Same for a film on MgO with chamber baking at p_N (f_N)= 71 mTorr (5.15 sccm). In this case T_C = 4.58 K.

direct effect of nitrogen incorporation was minimized. Some of the films were annealed. We see that a clear correlation exists between the T_C and both the Ti:N ratio and the oxygen content, with a low Ti:N ratio and low oxygen content both leading to strongly improving T_C values. Moreover, the sum of the oxygen and nitrogen contents in this whole set of samples stays constant at 53 at. % within the accuracy of the Tof-ERDA method. Thus, we conclude that oxygen displaces nitrogen in the films (Ti bonding more strongly to O), if it is allowed to be present during the deposition, and this extra oxygen is the critical deleterious ingredient which leads to degradation of the T_C. To put it another way, the dependence in Fig. 8 (a) is also due to oxygen, and not due to nitrogen.

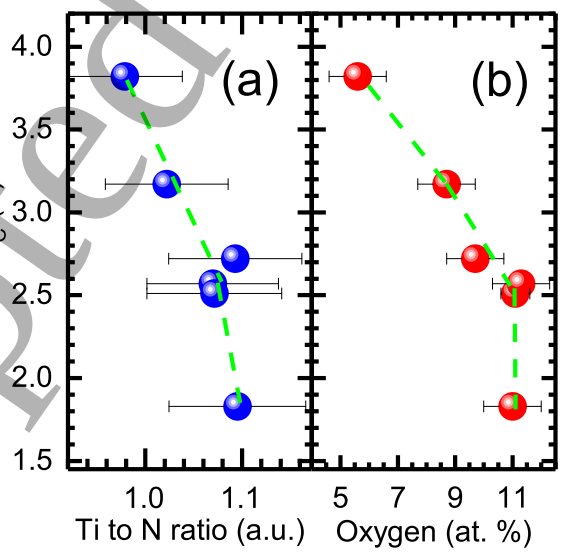

Figure 8. The correlation between the T_Cs and (a) the Ti:N ratio, and (b) the oxygen content within the film, for films deposited without chamber baking.

Accepted Manuscript

The strongly lowered oxygen impurity content must also be behind the much improved resistivity seen in films deposited with pre-baking (Fig 5 (b)). In addition, the fact that there was lack of T_C control with nitrogen pressure p_N in the case of non-baked chamber (Fig. 5 (a)) can now be understood as arising from variations of the additional oxygen contamination present in the chamber atmosphere during the deposition process. After introducing the better residual gas purification technique (pre-baking), a better trend of increasing T_C with nitrogen pressure was seen, with state-of-the-art high T_Cs, competitive with the best results obtained with sputtering.

In the films deposited with pre-baking and analyzed for elemental content, oxygen content was at or below 1 at. % and T_Cs were all above 4 K, consistent with Fig. 8. Due to the lowered oxygen levels, the nitrogen levels were all higher, between 55 – 60 at. %. Nevertheless, T_Cs remained high between 4 – 4.5 K showing that nitrogen-richness at that level is not detrimental to the superconducting properties. Further studies are required to further clarify the direct effect of nitrogen content in low-oxygen content films, and what caused the remaining variations of T_C in these films where oxygen impurities did not play a decisive role anymore.

4. Conclusions

In conclusion, we fabricated high-quality epitaxial superconducting titanium nitride thin films for the first time using a pulsed laser deposition technique, using an infrared solid-state Nd:YAG laser for this purpose. The films were deposited on magnesium oxide, sapphire and silicon nitride substrates at 700°C in a constant flow of nitrogen using a titanium target. The type of substrate did not have a strong effect on the superconducting properties. In the best film, superconducting transition temperature was as high as 4.8 K, higher than in most previous superconducting TiN films deposited with reactive sputtering [6, 35, 14, 34]. A low room temperature resistivity $\sim 17\mu\Omega$cm and RRR up to 3 were observed in the best film, approaching sputtered single crystal film levels [29, 36]. Clearly, PLD is a practical and versatile alternative to reactive sputtering for superconducting TiN film deposition.

For some films, Hall and magnetoresistance were also measured. The effective conduction electron density obtained from the Hall measurements was in agreement with the theoretical value, and the magnitude of longitudinal magnetoresistance was very low, ~ 0.05 % at ~ 1 T. The shape of the magnetoresistance curve was unusual, with a linear increase around zero field, and a saturation at fields above 1 T.

Elemental composition of several films was also analyzed with the help of Time-of-Flight Elastic Recoil Detection Analysis (ToF-ERDA), demonstrating a strong correlation between the oxygen impurity content, the T_C and ρ, with low oxygen content producing a higher T_C and a lower ρ. Without taking extra precautions, this oxygen content could be as high as ~ 10 at. %, showing the difficulty of working with such strong oxygen gettering material as Ti. By baking the deposition chamber in nitrogen flow for an extended time before each deposition, we managed to lower the oxygen

Accepted Manuscript

content to below 1 at. %, for which films the highest T_Cs were observed. Thus, strong measures to limit oxygen exposure of the films during the deposition must be taken to guarantee best superconducting film properties. Interestingly, in the films with low oxygen content, the nitrogen content could be highly overstoichiometric, with Ti/N ratios up to 40/ 60, without adverse effects on superconductivity, a fact not reported before. Low nitrogen content is known to suppress superconductivity [6, 35, 14], but it was not possible to make such highly nitrogen deficient films with out technique. This is actually positive, leading to fairly weak dependence of the film properties on the nitrogen flow rate, and thus lack of oversensitivity to the exact deposition conditions.

Structural analysis by X-ray diffraction was also performed on some films, showing that epitaxial growth on MgO was possible. Vacuum annealing was also shown to improve the crystallinity of films to some extent. However, our data did not indicate any strong correlations between crystal structure and superconducting properties, as polycrystalline films did sometimes exhibit higher T_Cs than epitaxial films. This is most likely because the structural studies were performed on films whose oxygen content was higher, and thus oxygen impurities were controlling the superconducting properties. Further studies on the level of crystalline quality and superconducting properties in low-oxygen-content films are required.

Acknowledgments

This research has been supported by Academy of Finland projects number 260880 and 298667 and Academy of Finland Center of Excellence in Nuclear and Accelerator Based Physics (Ref. 251353). We thank M. R. J. Palosaari and K. M. Kinnunen for assistance with low temperature measurements.

References

[1] R. Buhl, H.K. Pulker, and E. Moll. Tin coatings on steel. *Thin Solid Films*, 80(1):265 – 270, 1981.

[2] B. Zega, M. Kornmann, and J. Amiguet. Hard decorative tin coatings by ion plating. *Thin Solid Films*, 45(3):577 – 582, 1977.

[3] Y. Claesson, M. Georgson, A. Roos, and C.-G. Ribbing. Optical characterisation of titanium-nitride-based solar control coatings. *Solar Energy Materials*, 20(5):455 – 465, 1990.

[4] A. Sherman. Growth and properties of lpcvd titanium nitride as a diffusion barrier for silicon device technology. *Journal of The Electrochemical Society*, 137(6):1892–1897, 1990.

[5] R. Chau, S. Datta, M. Doczy, B. Doyle, J. Kavalieros, and M. Metz. High- kappa;/metal-gate stack and its mosfet characteristics. *IEEE Electron Device Letters*, 25(6):408–410, June 2004.

[6] Henry G. Leduc, Bruce Bumble, Peter K. Day, Byeong Ho Eom, Jiansong Gao, Sunil Golwala, Benjamin A. Mazin, Sean McHugh, Andrew Merrill, David C. Moore, Omid Noroozian, Anthony D. Turner, and Jonas Zmuidzinas. Titanium nitride films for ultrasensitive microresonator detectors. *Applied Physics Letters*, 97(10):102509, 2010.

[7] J. Gao, M. R. Vissers, M. O. Sandberg, F. C. S. da Silva, S. W. Nam, D. P. Pappas, D. S. Wisbey, E. C. Langman, S. R. Meeker, B. A. Mazin, H. G. Leduc, J. Zmuidzinas, and K. D. Irwin. A titanium-nitride near-infrared kinetic inductance photon-counting detector and its anomalous electrodynamics. *Applied Physics Letters*, 101(14):142602, 2012.

Accepted Manuscript

[8] P. Diener, H. G. Leduc, S. J. C. Yates, Y. J. Y. Lankwarden, and J. J. A. Baselmans. Design and testing of kinetic inductance detectors made of titanium nitride. *Journal of Low Temperature Physics*, 167(3):305–310, May 2012.

[9] Michael R. Vissers, Jiansong Gao, Martin Sandberg, Shannon M. Duff, David S. Wisbey, Kent D. Irwin, and David P. Pappas. Proximity-coupled ti/tin multilayers for use in kinetic inductance detectors. *Applied Physics Letters*, 102(23):232603, 2013.

[10] J. Bueno, P. C. J. J. Coumou, G. Zheng, P. J. de Visser, T. M. Klapwijk, E. F. C. Driessen, S. Doyle, and J. J. A Baselmans. Anomalous response of superconducting titanium nitride resonators to terahertz radiation. *Applied Physics Letters*, 105(19):192601, 2014.

[11] J. Hubmayr, J. Beall, D. Becker, H.-M. Cho, M. Devlin, B. Dober, C. Groppi, G. C. Hilton, K. D. Irwin, D. Li, P. Mauskopf, D. P. Pappas, J. Van Lanen, M. R. Vissers, Y. Wang, L. F. Wei, and J. Gao. Photon-noise limited sensitivity in titanium nitride kinetic inductance detectors. *Applied Physics Letters*, 106(7):073505, 2015.

[12] G. Coiffard, K.-F. Schuster, E. F. C. Driessen, S. Pignard, M. Calvo, A. Catalano, J. Goupy, and A. Monfardini. Uniform non-stoichiometric titanium nitride thin films for improved kinetic inductance detector arrays. *Journal of Low Temperature Physics*, 184(3):654–660, Aug 2016.

[13] M. R. Vissers, J. Gao, D. S. Wisbey, D. A. Hite, C. C. Tsuei, A. D. Corcoles, M. Steffen, and D. P. Pappas. Low loss superconducting titanium nitride coplanar waveguide resonators. *Applied Physics Letters*, 97(23):232509, 2010.

[14] S Ohya, B Chiaro, A Megrant, C Neill, R Barends, Y Chen, J Kelly, D Low, J Mutus, P J J O'Malley, P Roushan, D Sank, A Vainsencher, J Wenner, T C White, Y Yin, B D Schultz, C J Palmstrom, B A Mazin, A N Cleland, and John M Martinis. Room temperature deposition of sputtered tin films for superconducting coplanar waveguide resonators. *Superconductor Science and Technology*, 27(1):015009, 2014.

[15] Martin Sandberg, Michael R. Vissers, Thomas A. Ohki, Jiansong Gao, José Aumentado, Martin Weides, and David P. Pappas. Radiation-suppressed superconducting quantum bit in a planar geometry. *Applied Physics Letters*, 102(7):072601, 2013.

[16] Josephine B. Chang, Michael R. Vissers, Antonio D. Crcoles, Martin Sandberg, Jiansong Gao, David W. Abraham, Jerry M. Chow, Jay M. Gambetta, Mary Beth Rothwell, George A. Keefe, Matthias Steffen, and David P. Pappas. Improved superconducting qubit coherence using titanium nitride. *Applied Physics Letters*, 103(1):012602, 2013.

[17] K. Makise, R. Sun, H. Terai, and Z. Wang. Fabrication and characterization of epitaxial tin-based josephson junctions for superconducting circuit applications. *IEEE Transactions on Applied Superconductivity*, 25(3):1–4, June 2015.

[18] Francesco Giazotto, Tero T. Heikkilä, Arttu Luukanen, Alexander M. Savin, and Jukka P. Pekola. Opportunities for mesoscopics in thermometry and refrigeration: Physics and applications. *Rev. Mod. Phys.*, 78:217–274, Mar 2006.

[19] T. I. Baturina, A. Yu. Mironov, V. M. Vinokur, M. R. Baklanov, and C. Strunk. Localized superconductivity in the quantum-critical region of the disorder-driven superconductor-insulator transition in tin thin films. *Phys. Rev. Lett.*, 99:257003, Dec 2007.

[20] Valerii M. Vinokur, Tatyana I. Baturina, Mikhail V. Fistul, Aleksey Yu. Mironov, Mikhail R. Baklanov, and Christoph Strunk. Superinsulator and quantum synchronization. *Nature (London)*, 452:613–615, 2008.

[21] B. Sacépé, C. Chapelier, T. I. Baturina, V. M. Vinokur, M. R. Baklanov, and M. Sanquer. Disorder-induced inhomogeneities of the superconducting state close to the superconductor-insulator transition. *Phys. Rev. Lett.*, 101:157006, Oct 2008.

[22] Benjamin Sacépé, Claude Chapelier, Tatyana I. Baturina, Valerii M. Vinokur, Mikhail R. Baklanov, and Marc Sanquer. Pseudogap in a thin film of a conventional superconductor. *Nature Comm.*, 1:140, 2010.

[23] E. F. C. Driessen, P. C. J. J. Coumou, R. R. Tromp, P. J. de Visser, and T. M. Klapwijk. Strongly disordered tin and nbtin *s*-wave superconductors probed by microwave electrodynamics. *Phys.*

Accepted Manuscript

Rev. Lett., 109:107003, Sep 2012.

[24] P. C. J. J. Coumou, E. F. C. Driessen, J. Bueno, C. Chapelier, and T. M. Klapwijk. Electrodynamic response and local tunneling spectroscopy of strongly disordered superconducting tin films. *Phys. Rev. B*, 88:180505, Nov 2013.

[25] John R. Peterson. Partial pressure of ticl4 in cvd of tin. *Journal of Vacuum Science and Technology*, 11(4):715–718, 1974.

[26] S.R. Kurtz and R.G. Gordon. Chemical vapor deposition of titanium nitride at low temperatures. *Thin Solid Films*, 140(2):277 – 290, 1986.

[27] Alessandra Satta, Gerald Beyer, Karen Maex, Kai Elers, Suvi Haukka, and A. Vantomme. Properties of tin thin films deposited by alcvd as barrier for cu metallization. *MRS Proceedings*, 612, 2000.

[28] J.M. Poitevin, G. Lemperiere, and J. Tardy. Influence of substrate bias on the composition, structure and electrical properties of reactively d.c.-sputtered tin films. *Thin Solid Films*, 97(1):69 – 77, 1982.

[29] B. O. Johansson, J. E. Sundgren, J. E. Greene, A. Rockett, and S. A. Barnett. Growth and properties of single crystal tin films deposited by reactive magnetron sputtering. *Journal of Vacuum Science & Technology A: Vacuum, Surfaces, and Films*, 3(2):303–307, 1985.

[30] N. Biunno, J. Narayan, S. K. Hofmeister, A. R. Srivatsa, and R. K. Singh. Lowtemperature processing of titanium nitride films by laser physical vapor deposition. *Applied Physics Letters*, 54(16):1519–1521, 1989.

[31] O Auciello, T Barnes, S Chevacharoenkul, A.F Schreiner, and G.E McGuire. Laser ablation deposition of titanium nitride films on silicon substrates at room temperature. *Thin Solid Films*, 181(1):65 – 73, 1989. International Conference on Metallurgical Coatings, San Diego, 1989.

[32] P. C. J. J. Coumou, M. R. Zuiddam, E. F. C. Driessen, P. J. de Visser, J. J. A. Baselmans, and T. M. Klapwijk. Microwave properties of superconducting atomic-layer deposited tin films. *IEEE Transactions on Applied Superconductivity*, 23(3):7500404, June 2013.

[33] Andrii Torgovkin, Saumyadip Chaudhuri, Jari Malm, Timo Sajavaara, and Ilari J. Maasilta. Normal-metalinsulatorsuperconductor tunnel junction with atomic-layer-deposited titanium nitride as superconductor. *IEEE Transactions on Applied Superconductivity*, 25(3):1101604, 2015.

[34] H. M. I. Jaim, J. A. Aguilar, B. Sarabi, Y. J. Rosen, A. N. Ramanayaka, E. H. Lock, C. J. K. Richardson, and K. D. Osborn. Superconducting tin films sputtered over a large range of substrate dc bias. *IEEE Transactions on Applied Superconductivity*, 25(3):1–5, June 2015.

[35] Michael R. Vissers, Jiansong Gao, Jeffrey S. Kline, Martin Sandberg, Martin P. Weides, David S. Wisbey, and David P. Pappas. Characterization and in-situ monitoring of sub-stoichiometric adjustable superconducting critical temperature titanium nitride growth. *Thin Solid Films*, 548(Supplement C):485 – 488, 2013.

[36] R. Sun, K. Makise, W. Qiu, H. Terai, and Z. Wang. Fabrication of (200)-oriented tin films on si (100) substrates by dc magnetron sputtering. *IEEE Transactions on Applied Superconductivity*, 25(3):1–4, June 2015.

[37] Yoshiharu Krockenberger, Shin-ichi Karimoto, Hideki Yamamoto, and Kouich Semba. Coherent growth of superconducting tin thin films by plasma enhanced molecular beam epitaxy. *Journal of Applied Physics*, 112(8):083920, 2012.

[38] W. Spengler, R. Kaiser, A. N. Christensen, and G. Müller-Vogt. Raman scattering, superconductivity, and phonon density of states of stoichiometric and nonstoichiometric tin. *Phys. Rev. B*, 17:1095–1101, Feb 1978.

[39] J. Narayan, P. Tiwari, X. Chen, J. Singh, R. Chowdhury, and T. Zheleva. Epitaxial growth of tin films on (100) silicon substrates by laser physical vapor deposition. *Applied Physics Letters*, 61(11):1290–1292, 1992.

[40] R. Chowdhury, R. D. Vispute, K. Jagannadham, and J. Narayan. Characteristics of titanium

Accepted Manuscript

nitride films grown by pulsed laser deposition. *Journal of Materials Research*, 11(6):14581469, 1996.

[41] R. Timm, P. R. Willmott, and J. R. Huber. Parallel epitaxy of tin(100) thin films on si(100) produced by pulsed reactive crossed-beam laser ablation. *Applied Physics Letters*, 71(14):1966–1968, 1997.

[42] S. Xu, L. Du, K. Sugioka, K. Toyoda, and M. Jyumonji. Preferred growth of epitaxial tin thin film on silicon substrate by pulsed laser deposition. *Journal of Materials Science*, 33(7):1777–1782, Apr 1998.

[43] N. Biunno, J. Narayan, A. R. Srivatsa, and O. W. Holland. Laser deposition of epitaxial titanium nitride films on (100)mgo. *Applied Physics Letters*, 55(4):405–407, 1989.

[44] Kei Inumaru, Takayoshi Ohara, and Shoji Yamanaka. Pulsed laser deposition of epitaxial titanium nitride on mgo(001) monitored by rheed oscillation. *Applied Surface Science*, 158(3):375 – 377, 2000.

[45] V. Talyansky, S. Choopun, M.J. Downes, R. P. Sharma, T. Venkatesan, Y. X. Li, L. G. Salamanca-Riba, M. C. Wood, R. T. Lareau, K. A. Jones, and et al. Pulsed laser deposition of titanium nitride films on sapphire. *Journal of Materials Research*, 14(8):32983302, 1999.

[46] J.M. Lackner, W. Waldhauser, R. Berghauser, R. Ebner, B. Major, and T. Schöberl. Structural, mechanical and tribological investigations of pulsed laser deposited titanium nitride coatings. *Thin Solid Films*, 453-454(Supplement C):195 – 202, 2004. Proceedings of Symposium H on Photonic Processing of Surfaces, Thin Films and Devices, of the E-MRS 2003 Spring Conference.

[47] B. Major, W. Mróz, T. Wierzchon, W. Waldhauser, J. Lackner, and R. Ebner. Pulsed laser deposition of advanced titanium nitride thin layers. *Surface and Coatings Technology*, 180-181(Supplement C):580 – 584, 2004. Proceedings of Symposium G on Protective Coatings and Thin Films-03, of the E-MRS 2003 Spring Conference.

[48] S. Chaudhuri, M. R. Nevala, and I. J. Maasilta. Niobium nitride-based normal metal-insulator-superconductor tunnel junction microthermometer. *Applied Physics Letters*, 102(13):132601, 2013.

[49] P. Mikheenko, T. H. Johansen, S. Chaudhuri, I. J. Maasilta, and Y. M. Galperin. Ray optics behavior of flux avalanche propagation in superconducting films. *Phys. Rev. B*, 91:060507, Feb 2015.

[50] Saumyadip Chaudhuri, Ilari J. Maasilta, Lucie Chandernagor, Marion Ging, and Manu Lahtinen. Fabrication of superconducting tantalum nitride thin films using infrared pulsed laser deposition. *Journal of Vacuum Science & Technology A*, 31(6):061502, 2013.

[51] S. Chaudhuri and I. J. Maasilta. Superconducting tantalum nitride-based normal metal-insulator-superconductor tunnel junctions. *Applied Physics Letters*, 104(12):122601, 2014.

[52] S. Chaudhuri, M.R. Nevala, T. Hakkarainen, T. Niemi, and I.J. Maasilta. Infrared pulsed laser deposition of niobium nitride thin films. *IEEE Transactions on Applied Superconductivity*, 21(3):143–146, 2011.

[53] Mikko Laitinen, Mikko Rossi, Jaakko Julin, and Timo Sajavaara. Time-of-flight energy spectrometer for elemental depth profiling jyvskyl design. *Nuclear Instruments and Methods in Physics Research Section B: Beam Interactions with Materials and Atoms*, 337:55–61, Oct 2014.

[54] C.-S. Shin, S. Rudenja, D. Gall, N. Hellgren, T.-Y. Lee, I. Petrov, and J. E. Greene. Growth, surface morphology, and electrical resistivity of fully strained substoichiometric epitaxial tinx (0.67¡x¡1.0) layers on mgo(001). *Journal of Applied Physics*, 95(1):356–362, 2004.

[55] S. Chaudhuri, M. R. Nevala, T. Hakkarainen, T. Niemi, and I. J. Maasilta. Infrared pulsed laser deposition of niobium nitride thin films. *IEEE Transactions on Applied Superconductivity*, 21(3):143–146, June 2011.

[56] H. A. Wriedt and J. L. Murray. The n-ti (nitrogen-titanium) system. *Bulletin of Alloy Phase Diagrams*, 8(4):378–388, Aug 1987.

[57] D. Gall, I. Petrov, and J. E. Greene. Epitaxial sc1xtixn(001): Optical and electronic transport

Accepted Manuscript

properties. *Journal of Applied Physics*, 89(1):401–409, 2001.

[58] A. B. Pippard, editor. *Magnetoresistance in Metals*. Cambridge University Press, Cambridge, 1989.

Accepted Manuscript